Brain Pathology ISSN 1015–6305

MINI-SYMPOSIUM: ENERGY DEMAND AND ENERGY SUPPLY IN ALZHEIMER'S DISEASE

Longitudinal Positron Emission Tomography in Preventive Alzheimer's Disease Drug Trials, Critical Barriers from Imaging Science Perspective

Sepideh Shokouhi[1]; Desmond Campbell[1]; Aaron B. Brill[1]; Harry E. Gwirtsman[2]; The Alzheimer's Disease Neuroimaging Initiative*

[1] Department of Radiology & Radiological Sciences, Vanderbilt University Medical Center.
[2] Department of Psychiatry, Vanderbilt University Medical Center.

Keywords
amyloid-PET, FDG, longitudinal PET, preclinical AD, positron emission tomography.

Corresponding author:
Sepideh Shokouhi Ph.D., Assistant Professor of Radiology and Radiological Sciences, Vanderbilt University Institute of Imaging Science, 1161 21st Avenue South, Medical Center North, AA-1105, Nashville, TN 37232-2310 (E-mail: *sepideh.shokouhi@vanderbilt.edu*)

Received 08 June 2016
Accepted 16 June 2016

*Data used in preparation of this article were obtained from the Alzheimer's Disease Neuroimaging Initiative (ADNI) database (adni.loni.usc.edu). As such, the investigators within the ADNI contributed to the design and implementation of ADNI and/or provided data but did not participate in analysis or writing of this report. A complete listing of ADNI investigators can be found at: http://adni.loni.ucla.edu/wp-content/uploads/how_to_apply/ADNI_Acknowledgement_List.pdf.

The authors declare that they have no competing interests.

doi:10.1111/bpa.12399

Abstract

Recent Alzheimer's trials have recruited cognitively normal people at risk for Alzheimer's dementia. Due to the lack of clinical symptoms in normal population, conventional clinical outcome measures are not suitable for these early trials. While several groups are developing new composite cognitive tests that could serve as potential outcome measures by detecting subtle cognitive changes in normal people, there is a need for longitudinal brain imaging techniques that can correlate with temporal changes in these new tests and provide additional objective measures of neuropathological changes in brain. Positron emission tomography (PET) is a nuclear medicine imaging procedure based on the measurement of annihilation photons after positron emission from radiolabeled molecules that allow tracking of biological processes in body, including the brain. PET is a well-established *in vivo* imaging modality in Alzheimer's disease diagnosis and research due to its capability of detecting abnormalities in three major hallmarks of this disease. These include (1) amyloid beta plaques; (2) neurofibrillary tau tangles and (3) decrease in neuronal activity due to loss of nerve cell connection and death. While semiquantitative PET imaging techniques are commonly used to set discrete cut-points to stratify abnormal levels of amyloid accumulation and neurodegeneration, they are suboptimal for detecting subtle longitudinal changes. In this study, we have identified and discussed four critical barriers in conventional longitudinal PET imaging that may be particularly relevant for early Alzheimer's disease studies. These include within and across subject heterogeneity of AD-affected brain regions, PET intensity normalization, neuronal compensations in early disease stages and cerebrovascular amyloid deposition.

INTRODUCTION

Abnormal neurodegenerative processes in Alzheimer's disease (AD) begin many years before the clinical diagnosis of dementia, a phase that refers to as preclinical (presymptomatic) AD where individuals have little or no cognitive alterations to satisfy the diagnosis criteria for AD or mild cognitive impairment (MCI) (4, 26, 28, 31, 34, 36, 53, 62, 63, 66, 76, 79, 81). The National Institute on Aging-Alzheimer's Association workgroup (NIA-AA) has proposed three successive stages of preclinical AD (76). While common semiquantitative FDG-PET and amyloid beta (Aβ)-PET methods can stratify these stages (33, 39) by use of discrete cut-points for abnormal levels of Aβ (starting at stage 1) and neurodegeneration (starting at stage 2), there is considerably less experimental evidence about the rate of change in these biomarkers. There is a need for better understanding of the temporal progression of AD pathophysiology in preclinical phase that requires a more precise definition for testing new preventive therapeutic interventions. Recent Alzheimer's trials have recruited cognitively normal people at risk

for Alzheimer's dementia (77). Be caused by the lack of clinical symptoms in normal population, conventional clinical outcome measures, that is, time-to-AD conversion, may not be suitable for these early trials (1). While several groups are developing new composite cognitive tests that could serve as surrogate outcome measures by detecting subtle cognitive changes in normal people (2, 15), there is a need for longitudinal brain imaging techniques that can correlate with temporal changes in these new tests and provide additional objective measures of neuropathological changes in brain. In particular, within-individual longitudinal comparisons of imaging data may improve these evaluations by controlling for between subject variability. Several additional sources of variability need to be addressed and resolved to increase the accuracy of longitudinal measures of PET data. Previous research has addressed some of the biomedical and technical factors that could lead to variable PET imaging outcomes and made recommendations for controlling these parameters in longitudinal and cross-sectional studies. This article gives a summarized overview on the previous work and adds new points of consideration that are relevant to longitudinal PET imaging at preclinical stages of Alzheimer's disease.

MATERIALS AND METHODS

We reviewed 88 peer-reviewed articles dating from 1985 to 2016 to prepare this study. We searched these articles either directly in relevant journals or through PubMed database. In some cases, we also used imaging data as illustrative examples to support the cited literature.

Imaging data used in the preparation of this article were obtained from the Alzheimer's Disease Neuroimaging Initiative (ADNI) database (adni.loni.usc.edu). The ADNI was launched in 2003 as a public–private partnership, led by Principal Investigator Michael W. Weiner, MD. The primary goal of ADNI has been to test whether serial magnetic resonance imaging (MRI), positron emission tomography (PET), other biological markers, and clinical and neuropsychological assessment can be combined to measure the progression of mild cognitive impairment (MCI) and early Alzheimer's disease (AD).

CRITICAL BARRIERS IN LONGITUDINAL PET IMAGING

Within and across subject heterogeneity of affected brain regions in AD

FDG-PET

While from previous research, we know that AD hypometabolic regions include mainly posterior cingulate and parieto-temporal cortices (23, 35, 52, 70), there are also some differences among individual subjects (14, 41, 43). We refer to the study of Mosconi and colleagues (55) to provide illustrative and quantitative examples of differences in the topographic progression of hypometabolism across four cognitively normal older adults who eventually converted to AD, as verified by their post-mortem brain autopsy. Within this small cohort, we can see regional differences in the reduction of FDG-PET standardized uptake value ratio (SUVR) values. For example, some subjects develop initial hypometabolism in posterior cingulate cortex while others exhibit hypometabolism in temporal or parietal regions in addition to or without the posterior cingulate involvement. Some subjects show metabolic decline on both hemispheres whereas in others one side of the brain is more affected than the other side. This regional heterogeneity can complicate the evaluation of FDG-PET changes in a longitudinal study (e.g., drug evaluation). Previous research addressed this problem by defining composite regions of interest (ROIs) that included all AD signature areas (41, 45, 50). While this approach allows monitoring the same composite ROI for every subject (treats all subjects equally), it can attenuate the SUVR rate of change by averaging radiotracer activity values from rapidly changing regions with slower or nonchanging areas within the composite ROI. This will increase the variance of the SUVR mean value and reduce the longitudinal effect size.

Aβ-PET

Previous research (21, 22, 53, 68) has found that certain brain regions, such as the frontal, cingulate gyrus, precuneus and lateral parieto-temporal areas, show higher amyloid radiotracer uptake than other regions. Similar to the FDG-PET's composite ROI concept, many Aβ-PET studies calculate the mean SUVR value over these regions (sometimes over the entire neocortex), which is commonly referred to as the global cortical uptake. The global uptake has been used to classify subjects as amyloid positive or negative (33, 39) or to test the treatment efficacy of drugs (57, 64, 71). Similar to FDG-PET's AD-signature ROI, the cortical Aβ-PET SUVR mean values are associated with large standard errors (74). In a single subject, the SUVR standard deviation indicates voxel intensity variations across the global ROI. Even with the hypothetical presence of uniform radiotracer uptake, the voxel intensities would be subject to some variability that is characteristic of the PET scanner's noise performance. In Aβ-PET images, the radiotracer uptake is not uniform. There are additional voxel intensity variations due to specific (presence of classical Aβ plaques), nonspecific (retention in healthy tissue) and pseudo-specific (e.g., presence of cerebral amyloid angiopathy) (46) bindings. In a group of subjects, there is an additional across-subject variability in spatial uptake profiles due to variabilities in the Aβ patterns (85), even for those with similar total amyloid burden, as noted by Braak and Braak (4). We used Figure 1 to demonstrate regional differences in amyloid-PET uptake profile in two cognitively normal ADNI subjects (both amyloid positive).

Intensity normalization of PET images

While the "gold standard" for PET image quantitation necessitates full kinetic modeling with dynamic acquisition and arterial input function (56, 61), the semiquantitative SUVR metric is frequently used as a substitute method in clinical settings because it does not require long dynamic scans (subject to patient motion and discomfort) or the need to measure the arterial input function (invasive). The SUVR method calculates the ratio of the voxel intensity to a reference region intensity to correct for nonspecific radiotracer uptake and enables comparisons between different scans and subjects.

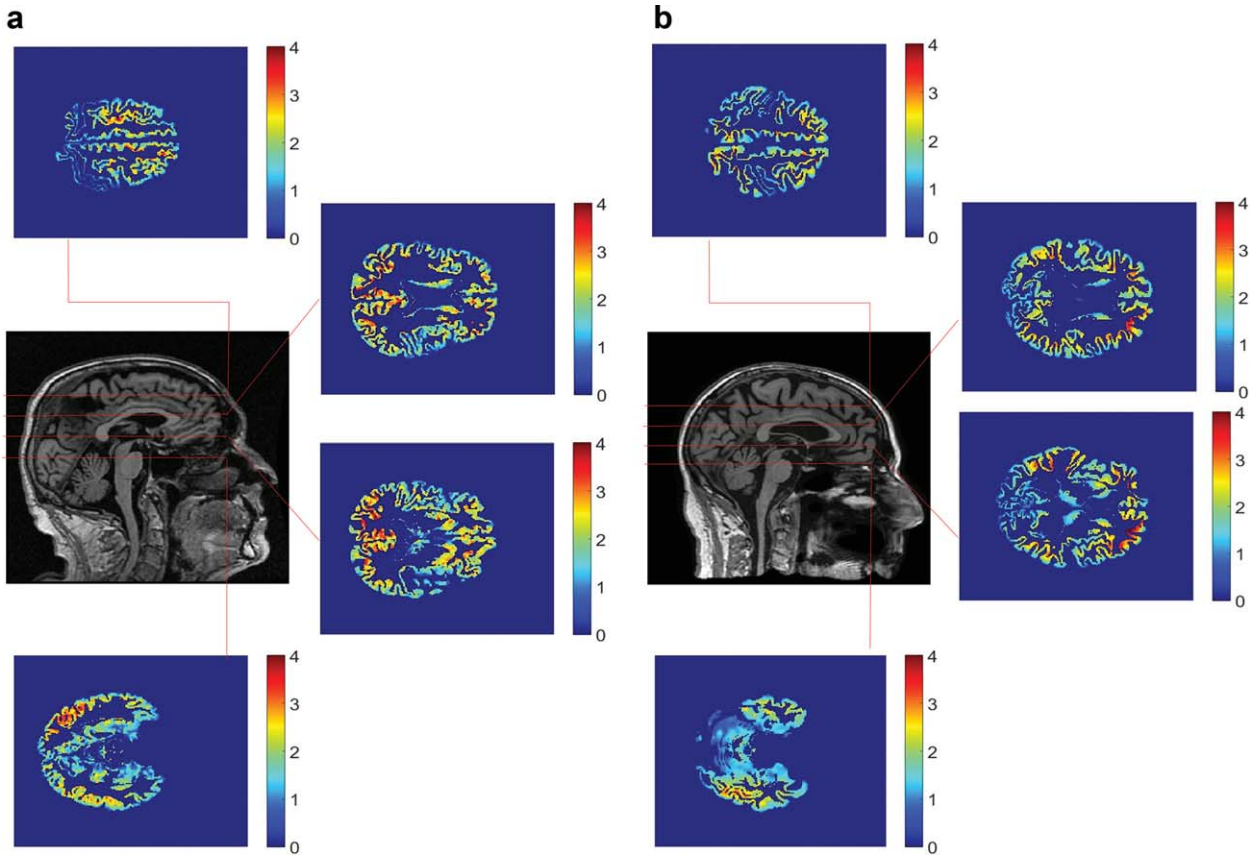

Figure 1. Two cognitively normal ADNI subjects imaged with [11C]PiB PET: We used 4 axial slices of their PET images (locations shown in corresponding MRI) to show differences in regional radiotracers uptake profiles.

FDG-PET

Different local and global normalization schemes are utilized in FDG-PET for brain studies and the selection of the optimal method has been debated (6, 16, 32, 51, 54). Ideally, metabolism in the reference region should be unaffected by AD. However, several non-AD conditions prevalent in elderly populations, such as brain injuries or vascular diseases could also alter the FDG uptake in a reference region (7, 42, 58). Given that approximately 30% of elderly people have silent infarcts without clinical manifestations (47), alterations in reference region metabolism are expected to occur in this aged population. We used Figure 2 to illustrate how longitudinal changes of regional FDG-PET SUVR values are affected by the reference region selection. This example shows longitudinal SUVR trajectories of two regions (posterior cingulate and occipital) in a cognitively normal ADNI subject. The SUVR trajectories are obtained by applying two different normalization schemes (pontine and cerebellar) to show how the selection of a reference region can change these trajectories. Global

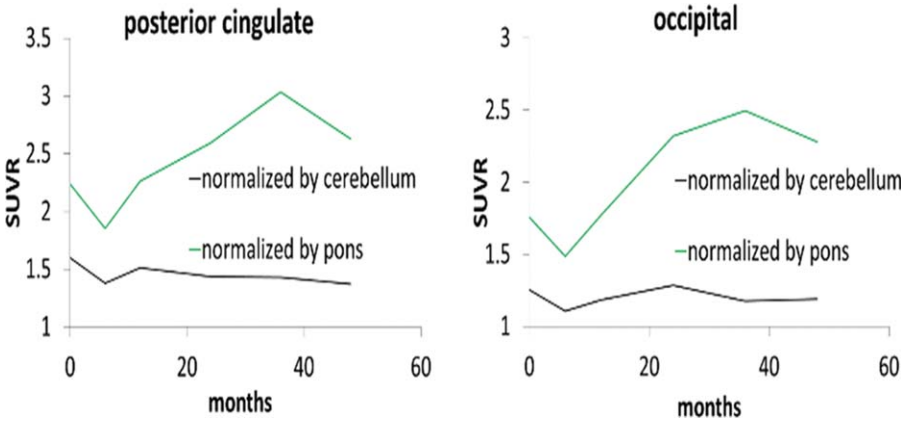

Figure 2. Mean FDG-PET SUVR values in a subject's posterior cingulate (left) and occipital lobe (right). For a given region, the cerebellar and pontine normalizations result in different trajectories (black and green) whereas the trajectories of two different regions normalized by the same reference region also look similar, indicating potential impact of reference region selection on SUVR trajectories.

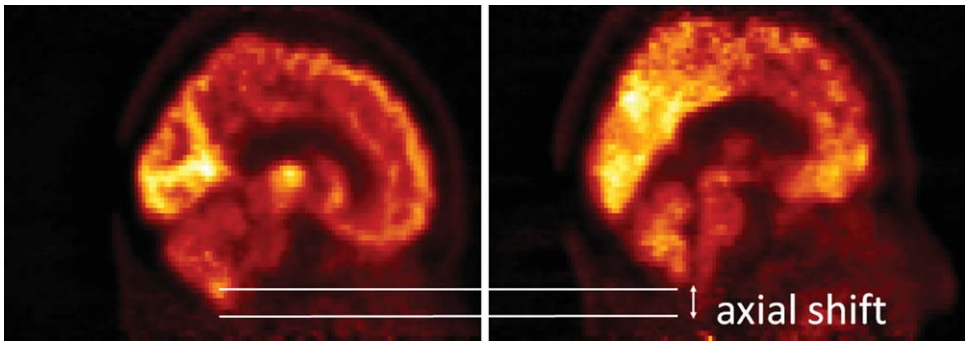

Figure 3. Two FDG-PET images acquired from an ADNI subject with slight shift in axial head position between baseline and follow-up.

normalization, where cerebral global mean is used to calculate the uptake ratio, has also found wide applications in FDG-PET studies of Alzheimer's disease. While the underlying rationale is that the global fluctuation in brain metabolism is not due to the changes produced by AD, local metabolic changes could contribute to the global signal variations, thus affecting this proportional scaling at both severe and early stages of the disease (84).

Aβ-PET

Similar to FDG-PET, semiquantitative SUVR values are used in clinical Aβ-PET image analyses with radiotracers, such as [^{11}C]PiB and [^{18}F]Florbetapir (8, 29, 48). As these radiotracers target predominately the classic cored and neuritic Aβ plaques, which are not frequently present in the cerebellum (11, 30, 37), the whole cerebellum or the cerebellar gray matter have served as reference regions for the majority of Aβ-PET studies to date. However, recent research (5, 10, 18, 44, 80, 83), including our own study (75), have raised concerns about the reliability of the cerebellar normalization for longitudinal [^{18}F]Florbetapir PET. It is not quite clear why the cerebellar normalization could be associated with increased variability of SUVR measures. Previous quantitative human Aβ-PET studies with [^{11}C]PiB (13, 17, 24, 40, 48, 61), [^{18}F]AZD4694 (67), [^{18}F]Florbetaben (3) and [^{18}F]Florbetapir (82) have clearly demonstrated low cerebellar retention in both AD and controls. It has been hypothesized that the axial location of the cerebellum, which increases the likelihood of scattered coincident events, and its shift between serial scans (Figure 3) may induce additional variability in cerebellar SUV (72). Clinical PET data undergo validated attenuation and scatter corrections to ensure quantitative accuracy across the field of view (86, 87). If the cerebellar axial position causes variable longitudinal measures, then it should be carefully evaluated with experimental studies to help improve the quality control of PET scans for brain studies. Pons/brainstem is another reference region that also falls often within the edges of the scanner's axial field-of-view, but appears to be a more stable reference region than cerebellum (75). For comparison, Landau and colleagues (44) found that using a combination of multiple reference regions, including the subcortical white matter and cerebellum and pons, into a composite reference region provides longitudinal changes that are biologically more plausible than trajectories obtained from cerebellar normalization alone. The reference region selection would be particularly important for monitoring earliest changes in Aβ-PET when the uptake ratio between target region and reference region is small, thus, more susceptible to potential variations.

Neuronal compensations in preclinical AD

There is an emerging evidence based on both FDG-PET (12) and functional MRI (19) that supports the existence of neural compensations in elderly people. The presence of positive correlation between metabolism and amyloid accumulation in early stages of the disease may indicate that the increased metabolism is a compensatory mechanism in the setting of initial AD pathology and a marker of impending neurodegeneration (12). Therefore, longitudinal PET analyses in preclinical AD should account for both abnormal increase and decrease of FDG-PET signals in different brain regions, thereby providing new ways of assessing disease progression in early stages where neuronal compensations are more likely present.

Cerebrovascular amyloid deposition

Previous studies with [^{11}C]PiB have detected elevated tracer uptake due to the contribution of cerebral amyloid angiopathy (CAA) in addition to the parenchymal amyloid (38, 46). CAA involves the deposition of β-amyloid in the media and adventitia of small and mid-sized cerebral arteries and veins (59). Under normal conditions, interstitial fluid and solutes drain from the brain parenchyma into cervical lymph nodes along basement membranes of small arteries, veins and capillaries by reverse transport, which is stimulated by the pulsatile flow in these vessels. The pathogenesis of CAA results from impaired clearance of β-amyloid peptides from the perivascular basement membranes, resulting in accumulation of these peptides in the cerebral vessels (20). CAA can be easily differentiated from parenchymal amyloid plaques in post-mortem tissue. However, *in vivo* image analytical methods have not as yet been developed for evaluating the development and relative contribution of CAA and parenchymal amyloid deposition to overall amyloid burden in AD brains studied longitudinally. CAA lesions can be found in 80%–85% of post-mortem brains of patients with AD and Down's Syndrome, and extensive CAA is seen in approximately half of AD patients (9). It is possible that both CAA and parenchymal amyloid contribute to the clinical AD progression (49). Additionally, APOE e2 and e4 alleles confer increased risk for CAA, as well as for AD (25, 60). Thus, CAA lesions may present an important factor in the pathogenesis of general amyloid deposition in the brain, and in the development of senile plaque formation. The ability to detect *CAA in vivo*, utilizing sophisticated

image analysis of Aβ-PET scans in individuals with mild neurocognitive impairment or normal individuals with subjective memory complaints (SMC), may improve our understanding of the contribution of CAA to overall brain amyloid deposition. Different AD drugs, that is, immunotherapies, may even increase the CAA, thus, preventing the complete removal of Aβ from brain (69). Current *in vivo* Aβ-PET imaging techniques cannot differentiate between parenchymal and vascular amyloid accumulations. Therefore, it is important to find new ways to evaluate the progression of these two co-occurring pathologies during the course of Alzheimer's disease and in response to treatments.

DISCUSSION

While early AD drug trials hold the promise of slowing abnormal disease processes before the onset of irreversible brain damage, the evaluation of their efficacy can be challenging due to the absence of clinical symptoms in tested subjects. Longitudinal imaging studies are becoming increasingly important to make objective assessments of abnormal changes in brain. Both Aβ-PET and FDG-PET are used in AD drug trials. Current longitudinal FDG-PET findings correlate well with clinical outcomes and cognitive tests of subjects with Alzheimer's dementia and mild cognitive impairment (45, 73, 78). There is a need for imaging studies that can find similar associations between PET measures and subtle cognitive alterations in normal\preclinical AD population. This is a challenging task because longitudinal imaging measures are subject to different sources of variability. The Influence of technical and biological factors on Aβ-PET and FDG-PET imaging in Alzheimer's disease has been discussed previously (17, 27, 72). This review gives a summarized overview on the previous work and added new points of consideration that are relevant to longitudinal PET imaging at preclinical stages of Alzheimer's disease.

Some of the FDG-PET related critical barriers were addressed in our previous studies where we developed a new technique for FDG-PET analysis, the regional FDG-PET time correlation coefficient (rFTC) (73) that measures similarities (correlations) between subject's serial scans. The correlation analysis can be performed on clinically acquired PET data (short static PET scans) and the correlation decline can be used as a marker of metabolic changes occurring anywhere in the brain. Therefore, this method provides a trajectory of metabolic changes using a single variable without the restriction of monitoring FDG changes in a single region or averaging FDG activities from multiple regions into a composite activity value. The correlation calculation does not require normalized PET images and the decline is triggered by both increases and decreases in brain metabolism, thus, providing a unique way of assessing the disease progression at the earliest stages where neuronal compensations can occur as early adapting mechanisms to the pathology. In comparison to region-based analyses, voxel-based methods do not require composite ROIs, and they can be applied on FDG-PET (52) and Aβ-PET (88). However, these techniques require the provision of means and standard deviations from a normal reference population (heterogeneity in reference population) to calculate the corresponding z-scores of the brain voxels. Finding a reference population for preclinical AD studies where test subjects are cognitively normal can be challenging. Also, voxel-based methods are typically performed on smoothed PET images that are spatially transformed into a template space. While these preprocessing steps enable cross-sectional comparisons as well as enhance the uniformity of PET images for qualitative assessments, their utility in longitudinal within-subject comparisons is debatable due to potential loss of image information (72). Regional analyses can be calculated in subject's native space. By selecting specific regions, they may provide more sensitive measures than global cortical averages (65, 85). Our group has also developed an alternative method to regional and voxel-based methods that enables monitoring different subjects with different topographic Aβ-PET radiotracer uptake profiles without averaging the voxel values (regional analysis) or requiring a reference population (voxel-based analysis). This method (74) is based on two-point correlation functions that capture longitudinal changes in Aβ-PET by detecting subtle changes in spatial radiotracer uptake patterns that are referred to as increased clustering or flocculence.

ACKNOWLEDGMENTS

Data collection and sharing for this project was funded by the Alzheimer's Disease Neuroimaging Initiative (ADNI) (National Institutes of Health Grant U01 AG024904) and DOD ADNI (Department of Defense award number W81XWH-12-2-0012). ADNI is funded by the National Institute on Aging, the National Institute of Biomedical Imaging and Bioengineering, and through generous contributions from the following: AbbVie, Alzheimer's Association; Alzheimer's Drug Discovery Foundation; Araclon Biotech; BioClinica, Inc.; Biogen; Bristol-Myers Squibb Company; CereSpir, Inc.; Cogstate; Eisai Inc.; Elan Pharmaceuticals, Inc.; Eli Lilly and Company; EuroImmun; F. Hoffmann-La Roche Ltd and its affiliated company Genentech, Inc.; Fujirebio; GE Healthcare; IXICO Ltd.; Janssen Alzheimer Immunotherapy Research & Development, LLC.; Johnson & Johnson Pharmaceutical Research & Development LLC.; Lumosity; Lundbeck; Merck & Co., Inc.; Meso Scale Diagnostics, LLC.; NeuroRx Research; Neurotrack Technologies; Novartis Pharmaceuticals Corporation; Pfizer Inc.; Piramal Imaging; Servier; Takeda Pharmaceutical Company; and Transition Therapeutics. The Canadian Institutes of Health Research is providing funds to support ADNI clinical sites in Canada. Private sector contributions are facilitated by the Foundation for the National Institutes of Health (www.fnih.org). The grantee organization is the Northern California Institute for Research and Education, and the study is coordinated by the Alzheimer's Therapeutic Research Institute at the University of Southern California. ADNI data are disseminated by the Laboratory for Neuro Imaging at the University of Southern California. ADNI data are disseminated by the Laboratory for Neuro Imaging at the University of Southern California. This study was supported by NIH grants R00 EB 009106, to S.Sh.

REFERENCES

1. Aisen PS, Andrieu S, Sampaio C, Carrillo M, Khachaturian ZS, Dubois B, Feldman HH, Petersen RC, Siemers E, Doody RS, Hendrix SB, Grundman M, Schneider LS, Schindler RJ, Salmon E, Potter WZ, Thomas RG, Salmon D, Donohue M, Bednar MM, Touchon J, Vellas B. (2011) Report of the task force on designing clinical trials in early (predementia) AD. *Neurology* **76**:280–286.

2. Ayutyanont N, Langbaum JB, Hendrix SB, Chen K, Fleisher AS, Friesenhahn M, Ward M, Aguirre C, Acosta-Baena N, Madrigal L, Muñoz C, Tirado V, Moreno S, Tariot PN, Lopera F, Reiman EM. (2014) The Alzheimer's prevention initiative composite cognitive test score: sample size estimates for the evaluation of preclinical Alzheimer's disease treatments in presenilin 1 E280A mutation carriers. *J Clin Psychiatry* **75**:652–660.
3. Becker GA, Ichise M, Barthel H, Luthardt J, Patt M, Seese A, Schultze-Mosgau M, Rohde B, Gertz HJ, Reininger C, Sabri O (2013) PET quantification of 18F-florbetaben binding to β-amyloid deposits in human brains. *J Nucl Med* **54**:723–731.
4. Braak H, Braak E (1991) Neuropathological stageing of Alzheimer-related changes. *Acta Neuropathol* **82**:239–259.
5. Brendel M, Högenauer M, Delker A, Sauerbeck J, Bartenstein P, Seibyl J, Rominger A, Alzheimer's Disease Neuroimaging Initiative (2015) Improved longitudinal [(18)F]-AV45 amyloid PET by white matter reference and VOI-based partial volume effect correction. *Neuroimage* **108**:450–459.
6. Buchert R, Wilke F, Chakrabarti B, Martin B, Brenner W, Mester J, Clausen M. (2005) Adjusted scaling of FDG positron emission tomography images for statistical evaluation in patients with suspected Alzheimer's disease. *J Neuroimaging* **15**:348–355.
7. Byrnes KR, Wilson CM, Brabazon F, von Leden R, Jurgens JS, Oakes TR, Selwyn RG (2014) FDG-PET imaging in mild traumatic brain injury: a critical review. *Front Neuroenergetics* **5**:13.
8. Camus V, Payoux P, Barré L, Desgranges B, Voisin T, Tauber C *et al* (2012) Using PET with 18F-AV-45 (florbetapir) to quantify brain amyloid load in a clinical environment. *Eur J Nucl Med Mol Imaging.* **39**(4):621–631.
9. Cano LM, Martinez-Yelamos S, Majos C, Alberti MA, Boluda S, Velasco R *et al* (2010) Reversible acute leukoencephalopathy as a form of presentation in cerebral amyloid angiopathy. *J Neurol Sci.* **288**: 190–193.
10. Chen K, Roontiva A, THiyyagura P, Lee W, Liu X, Ayutyanont N *et al* (2015) Improved power to characterize longitudinal amyloid-β PET changes and evaluate amyloid-modifying treatments using a cerebral white matter reference region. *J Nucl Med.* **56**(4):560–566.
11. Choi SR, Schneider JA, Bennett DA, Beach TG, Bedell BJ, Zehntner SP *et al* (2012) Correlation of amyloid PET ligand florbetapir F 18 (18F-AV-45) binding with β-amyloid aggregation and neuritic plaque deposition in postmortem brain tissue. *Alzheimer Disease and Associated Disorders.* **26**(1):8–16.
12. Cohen AD, Price JC, Weissfeld LA, James J, Rosario BL, Bi W *et al* (2009) Basal cerebral metabolism may modulate the cognitive effects of Ab in mild cognitive impairment: an example of brain reserve. *J Neurosci* **29**:14770–14778.
13. Cohen AD, Rabinovici GD, Mathis CA, Jagust WJ, Klunk WE, Ikonomovic MD (2012) Using Pittsburgh Compound B for in vivo PET imaging of fibrillar amyloid-beta. *Adv Pharmacol* **64**:27–81.
14. Del Sole A, Clerici F, Chiti A, Lecchi M, Mariani C, Maggiore L *et al* (2008) Individual cerebral metabolic deficits in Alzheimer's disease and amnestic mild cognitive impairment: an FDG PET study. *Eur J Nucl Med Mol Imaging* **35**:1357–1366.
15. Donohue MC, Sperling RA, Salmon DP, Rentz DM, Raman R, Thomas RG Australian Imaging, Biomarkers, and Lifestyle Flagship Study of Ageing; Alzheimer's Disease Neuroimaging Initiative; Alzheimer's Disease Cooperative Study. (2014) The preclinical Alzheimer cognitive composite: measuring amyloid-related decline. *JAMA Neurol.* **71**(8):961–970.
16. Dukart J, Mueller K, Horstmann A, Vogt B, Frisch S, Barthel H *et al* (2010) Differential effects of global and cerebellar normalization on detection and differentiation of dementia in FDG-PET studies. *Neuroimage* **49**:1490–1495.
17. Edison P, Hinz R, Brooks DJ (2011) Technical aspects of amyloid imaging for Alzheimer's disease. *Alzheimers Res Ther* **3**:25.
18. Edison P, Hinz R, Ramlackhansingh A, Thomas J, Gelosa G, Archer HA *et al* (2012) Can target-to-pons ratio be used as a reliable method for the analysis of [11C]PIB brain scans? *Neuroimage* **60**: 1716–1723.
19. Elman JA, Oh H, Madison CM, Baker SL, Vogel JW, Marks SM *et al* (2014) Neural compensation in older people with brain amyloid-β deposition. *Nat Neurosci* **17**:1316–1318.
20. Eng JA, Frosch MP, Choi K, Rebeck GW, Greenberg SM. (2004) Clinical manifestations of cerebral amyloid angiopathy-related inflammation. *Ann Neurol.* **55**(2):250–6.
21. Engler H, Forsberg A, Almkvist O, Blomquist G, Larsson E, Savitcheva I *et al* (2006) "Two-year follow-up of amyloid deposition in patients with Alzheimer's disease." *Brain* **129.11**: 2856–2866.
22. Forsberg A, Engler H, Almkvist O, Blomquist G, Hagman G, Wall A *et al* (2008) PET imaging of amyloid deposition in patients with mild cognitive impairment. *Neurobiol Aging* **29**:1456–1465.
23. Friedland RP, Budinger TF, Ganz E, Yano Y, Mathis CA, Koss B *et al* (1983) Regional cerebral metabolic alterations in dementia of the Alzheimer type: positron emission tomography with [18F]fluorodeoxyglucose. *J Comput Assist Tomogr.* **7**(4):590–598.
24. Gjedde A, Aanerud J, Braendgaard H, Rodell AB (2013) Blood-brain transfer of Pittsburgh compound B in humans. *Front Aging Neurosci* **5**:70.
25. Greenberg SM (1998) Cerebral amyloid angiopathy: prospects for clinical diagnosis and treatment. *Neurology* **51**:690–694.
26. Hardy J, Selkoe DJ (2002) The amyloid hypothesis of Alzheimer's disease: progress and problems on the road to therapeutics. *Science* **297**:353–356.
27. Herholz K (2012) Use of FDG PET as an imaging biomarker in clinical trials of Alzheimer's disease. *Biomark Med* **6**:431–439.
28. Holtzman DM, Morris JC, Goate AM (2011) Alzheimer's disease: the challenge of the second century. *Sci Transl Med* **3**:77sr71.
29. Huang KL, Lin KJ, Hsiao IT, Kuo HC, Hsu WC, Chuang WL *et al* (2013) Regional Amyloid Deposition in Amnestic Mild Cognitive Impairment and Alzheimer's Disease Evaluated by [18F]AV-45 Positron Emission Tomography in Chinese Population. Herholz K, ed. *PLoS ONE.* **8**(3):e58974.
30. Ikonomovic MD, Klunk WE, Abrahamson EE, Mathis CA, Price JC, Tsopelas ND *et al* (2008) Post-mortem correlates of in vivo PiB-PET amyloid imaging in a typical case of Alzheimer's disease. *Brain* **131**: 1630–1645.
31. Ingelsson M, Fukumoto H, Newell KL, Growdon JH, Hedley-Whyte ET, Frosch MP *et al* (2004) Early Abeta accumulation and progressive synaptic loss, gliosis, and tangle formation in AD brain. *Neurology* **62**: 925–931. 23;
32. Ishii K, Sasaki M, Kitagaki H, Yamaji S, Sakamoto S, Matsuda K, Mori E (1997) Reduction of cerebellar glucose metabolism in advanced Alzheimer's disease. *J Nucl Med* **38**:925–928.
33. Jack CR Jr, Knopman DS, Weigand SD, Wiste HJ, Vemuri P, Lowe V *et al* (2012) An operational approach to National Institute on Aging-Alzheimer's Association criteria for preclinical Alzheimer disease. *Ann Neurol* **71**:765–775.
34. Jack CR Jr, Lowe VJ, Weigand SD, Wiste HJ, Senjem ML, Knopman DS *et al* (2009) Serial PIB and MRI in normal, mild cognitive impairment and Alzheimer's disease: implications for sequence of pathological events in Alzheimer's disease. *Brain* **132**:1355–1365.
35. Jagust WJ, Friedland RP, Budinger TF (1985) Positron emission tomography with [18F]fluorodeoxyglucose differentiates normal pressure hydrocephalus from Alzheimer-type dementia. *J Neurol Neurosurg Psychiatry* **48**:1091–1096.

36. Jagust W, Gitcho A, Sun F, Kuczynski B, Mungas D, Haan M (2006) Brain imaging evidence of preclinical Alzheimer's disease in normal aging. *Ann Neurol* **59**:673–681.
37. Joachim CL, Morris JH, Selkoe DJ (1989) Diffuse senile plaques occur commonly in the cerebellum in Alzheimer's disease. *Am J Pathol* **135**: 309–319.
38. Johnson KA, Gregas M, Becker JA, Kinnecom C, Salat DH, Moran EK *et al* (2007) Imaging of amyloid burden and distribution in cerebral amyloid angiopathy. *Ann Neurol* **62**:229–234.
39. Johnson K, Sperling R, Gidicsin C, Carmasin JS, Maye JE, Coleman RE *et al* (2013) Florbetapir (F18-AV-45) PET to assess amyloid burden in Alzheimer's disease dementia, mild cognitive impairment, and normal aging. Alzheimer's *& dementia: the journal of the Alzheimer's Association.* **9**(0):S72–S83.
40. Klunk WE, Engler H, Nordberg A, Wang Y, Blomqvist G, Holt DP *et al* (2004) Imaging brain amyloid in Alzheimer's disease with Pittsburgh Compound-B. *Ann Neurol.* **55**:306–319.
41. Knopman DS, Jack CR Jr, Wiste HJ, Lundt ES, Weigand SD, Vemuri P *et al* (2014) 18F-fluorodeoxyglucose positron emission tomography, aging, and apolipoprotein E genotype in cognitively normal persons. *Neurobiol Aging.* **35**(9): 2096–106.
42. Kushner M, Tobin M, Alavi A, Chawluk J, Rosen M, Fazekas F *et al* (1987) Cerebellar glucose consumption in normal and pathologic states using fluorine-FDG and PET. *J Nucl Med* **28**:1667–1670.
43. Lam B, Masellis M, Freedman M, Stuss DT, Black SE (2013) Clinical, imaging, and pathological heterogeneity of the Alzheimer's disease syndrome. *Alzheimers Res Ther* **5**:1.
44. Landau SM, Fero A, Baker SL2, Koeppe R, Mintun M, Chen K *et al* (2015) Measurement of Longitudinal β-Amyloid Change with 18F-Florbetapir PET and Standardized Uptake Value Ratios. *J Nucl Med* **56**:567–574.
45. Landau SM, Harvey D, Madison CM, Koeppe RA, Reiman EM, Foster NL *et al* (2011) Associations between cognitive, functional, and FDG-PET measures of decline in AD and MCI. *Neurobiol Aging* **32**: 1207–1218.
46. Lockhart A, Lamb JR, Osredkar T, Sue LI, Joyce JN, Ye L *et al* (2007) PIB is a non-specific imaging marker of amyloid-beta (Abeta) peptide-related cerebral amyloidosis. *Brain* **130**:2607–2615.
47. Longstreth WT, Jr, Bernick C, Manolio TA, Bryan N, Jungreis CA, Price TR (1998) Lacunar infarcts defined by magnetic resonance imaging of 3660 elderly people: the cardiovascular health study. *Arch Neurol* **55**:1217–1225.
48. Lopresti BJ, Klunk WE, Mathis CA, Hoge JA, Ziolko SK, Lu X *et al* (2005) Simplified quantification of Pittsburgh Compound B amyloid imaging PET studies: a comparative analysis. *J Nucl Med* **46**: 1959–1972.
49. Love S, Miners S, Palmer J, Chalmers K, Kehoe P (2009) Insights into the pathogenesis and pathogenicity of cerebral amyloid angiopathy. *Front Biosci* **14**:4778–4792.
50. Lowe VJ, Weigand SD, Senjem ML, Vemuri P, Jordan L, Kantarci K *et al* (2014) Association of hypometabolism and amyloid levels in aging, normal subjects. *Neurology* **82**:1959–1967.
51. Minoshima S, Frey KA, Foster NL, Kuhl DE (1995) Preserved pontine glucose metabolism in Alzheimer disease: a reference region for functional brain image (PET) analysis. *J Comput Assist Tomogr* **19**: 541–547.
52. Minoshima S, Giordani B, Berent S, Frey KA, Foster NL, Kuhl DE (1997) Metabolic reduction in the posterior cingulate cortex in very early Alzheimer's disease. *Ann. Neurol* **42**:85–94.
53. Mintun MA, Larossa GN, Sheline YI, Dence CS, Lee SY, Mach RH *et al* (2006) [11C]PIB in a nondemented population: potential antecedent marker of Alzheimer disease. *Neurology* **67**:446–452.
54. Mosconi L (2013) Glucose metabolism in normal aging and Alzheimer's disease: methodological and physiological considerations for PET studies. *Clin Transl Imaging* **1**:
55. Mosconi L, Mistur R, Switalski R, Tsui WH, Glodzik L, Li Y *et al* (2009) FDG-PET changes in brain glucose metabolism from normal cognition to pathologically verified Alzheimer's disease. *Eur J Nucl Med Mol Imaging* **36**:811–822.
56. Mosconi L, Tsui WH, Rusinek H, De Santi S, Li Y, Wang GJ *et al* (2007) Quantitation, regional vulnerability, and kinetic modeling of brain glucose metabolism in mild Alzheimer's disease. *Eur J Nucl Med Mol Imaging* **34**:1467–1479.
57. Ostrowitzki S, Deptula D, Thurfjell L, Barkhof F, Bohrmann B, Brooks DJ *et al* (2012) Mechanism of amyloid removal in patients with Alzheimer disease treated with Gantenerumab. *Arch Neurol* **69**:198–207.
58. Peskind ER, Petrie EC, Cross DJ, Pagulayan K, McCraw K, Hoff D *et al* (2011) Cerebrocerebellar hypometabolism associated with repetitive blast exposure mild traumatic brain injury in 12 Iraq war Veterans with persistent post-concussive symptoms. *Neuroimage* **54**(Suppl.1):S76–S82.
59. Pezzini A, Del Zotto E, Volonghi I, Giossi A, Costa P, Padovani A (2009) Cerebral amyloid angiopathy: a common cause of cerebral hemorrhage. *Curr Med Chem* **16**:2498–2513.
60. Premkumar DR, Cohen DL, Hedera P, Friedland RP, Kalaria RN (1996) Apolipoprotein E-ϵ4 alleles in cerebral amyloid angiopathy and cerebrovascular pathology associated with Alzheimer's disease. *Am J Pathol* **148**:2083–2095.
61. Price JC, Klunk WE, Lopresti BJ, Lu X, Hoge JA, Ziolko SK *et al* (2005) Kinetic modeling of amyloid binding in humans using PET imaging and Pittsburgh Compound-B. *J Cereb Blood Flow Metab* **25**: 1528–1547.
62. Price JL, Morris JC (1999) Tangles and plaques in nondemented aging and "preclinical" Alzheimer's disease. *Ann Neurol* **45**:358–368.
63. Reiman EM, Caselli RJ, Yun LS, Chen K, Bandy D, Minoshima S *et al* (1996) Preclinical evidence of Alzheimer's disease in persons homozygous for the ϵ4 allele for apolipoprotein E. *N. Engl. J. Med.* **334**(12): 752–8.
64. Rinne JO, Brooks DJ, Rossor MN, Fox NC, Bullock R, Klunk WE *et al* (2010) 11C-PiB PET assessment of change in fibrillar amyloid-beta load in patients with Alzheimer's disease treated with bapineuzumab: a phase 2, double-blind, placebo-controlled, ascending-dose study. *Lancet Neurol* **9**:363–372.
65. Rodrigue KM, Kennedy KM, Devous MD Sr, Rieck JR, Hebrank AC, Diaz-Arrastia R *et al* (2012) β-Amyloid burden in healthy aging: regional distribution and cognitive consequences. *Neurology* **78**: 387–395.
66. Rowe CC, Ellis KA, Rimajova M, Bourgeat P, Pike KE, Jones G *et al* (2010) Amyloid imaging results from the Australian imaging, biomarkers and lifestyle (AIBL) study of aging. *Neurobiol Aging* **31**: 1275–1283.
67. Rowe CC, Pejoska S, Mulligan RS, Jones G, Chan JG, Svensson S *et al* (2013) Head-to-head comparison of 11C-PiB and 18F-AZD4694 (NAV4694) for β-amyloid imaging in aging and dementia. *J Nucl Med* **54**:880–886.
68. Rowe CC, Villemagne VL (2011) Brain amyloid imaging. *J Nucl Med* **52**:1733–1740.
69. Weller RO, Preston SD, Subash M, Carare RO (2009) Cerebral amyloid angiopathy in the aetiology and immunotherapy of Alzheimer disease. *Alzheimers Res Ther* **1**:6–13.
70. Salmon E, Collette F, Degueldre C, Lemaire C, Franck G (2000) Voxel-based analysis of confounding effects of age and dementia severity on cerebral metabolism in Alzheimer's disease. *Human Brain Mapping* **10**:39–48.

71. Salloway S, Sperling R, Fox NC, Blennow K, Klunk W, Raskind M *et al* (2014) Two phase 3 trials of bapineuzumab in mild-to-moderate Alzheimer's disease. *N Engl J Med* **370**:322–333.
72. Schmidt ME, Chiao P, Klein G, Matthews D, Thurfjell L, Cole PE *et al* (2015) The influence of biological and technical factors on quantitative analysis of amyloid PET: Points to consider and recommendations for controlling variability in longitudinal data. *Alzheimers Dement.* **11**:1050–1068.
73. Shokouhi S, Claassen D, Kang H, Ding Z, Rogers B, Mishra A, Riddle WR (2013) Longitudinal progression of cognitive decline correlates with changes in the spatial pattern of brain 18F-FDG PET. *J Nucl Med* **54**:1564–1569.
74. Shokouhi S, Rogers BP, Kang H, Ding Z, Claassen DO, Mckay JW, Riddle WR (2015) Modeling clustered activity increase in amyloid-beta positron emission tomographic images with statistical descriptors. *Clin Interv Aging* **20**:759–770.
75. Shokouhi S, Mckay JW, Baker SL, Kang H, Brill AB, Gwirtsman HE *et al* (2016) Reference tissue normalization in longitudinal 18F-florbetapir positron emission tomography of late mild cognitive impairment. *Alzheimers Res Therapy* **8**:2.
76. Sperling RA, Aisen PS, Beckett LA, Bennett DA, Craft S, Fagan AM, Iwatsubo T *et al* (2011) Toward defining the preclinical stages of Alzheimer's disease: recommendations from the national institute on aging-Alzheimer's association workgroups on diagnostic guidelines for Alzheimer's disease. *Alzheimers Dement* **7**:280–292.
77. Sperling RA, Rentz DM, Johnson KA, Karlawish J, Donohue M, Salmon DP, Aisen P (2014) The A4 study: stopping AD before symptoms begin? *Sci Transl Med* **6**:228fs13.
78. Stefanova E, Wall A, Almkvist O, Nilsson A, Forsberg A, Långström B, Nordberg A (2006) Longitudinal PET evaluation of cerebral glucose metabolism in rivastigmine treated patients with mild Alzheimer's disease. *J Neural Transm* **113**:205–218.
79. Thal DR, von Arnim C, Griffin WS, Yamaguchi H, Mrak RE, Attems J, Upadhaya AR (2013) Pathology of clinical and preclinical Alzheimer's disease. *Eur Arch Psychiatry Clin Neurosci* **263(Suppl.2)**: S137–S145.
80. Tryputsen V, DiBernardo A, Samtani M, Novak GP, Narayan VA, Raghavan N (2015) Alzheimer's disease neuroimaging initiative. Optimizing regions-of-interest composites for capturing treatment effects on brain amyloid in clinical trials. *J Alzheimers Dis* **43**:809–821.
81. Vlassenko AG, Benzinger TL, Morris JC (2012) PET amyloid-beta imaging in preclinical Alzheimer's disease. *Biochim Biophys Acta* **1822**:370–379.
82. Wong DF, Rosenberg PB, Zhou Y, Kumar A, Raymont V, Ravert HT *et al* (2010) In vivo imaging of amyloid deposition in Alzheimer disease using the radioligand 18F-AV-45 (florbetapir [corrected] F 18). *J Nucl Med* **51**:913–920.
83. Wong KP, Wardak M, Shao W, Dahlbom M, Kepe V, Liu J *et al* (2010) Quantitative analysis of [18F]FDDNP PET using subcortical white matter as reference region. *Eur J Nucl Med Mol Imaging* **37**: 575–588.
84. Yakushev I, Landvogt C, Buchholz HG, Fellgiebel A, Hammers A, Scheurich A *et al* (2008) Choice of reference area in studies of Alzheimer's disease using positron emission tomography with fluorodeoxyglucose-F18. *Psychiatry Res* **164**:143–153.
85. Yotter RA, Doshi J, Clark V, Sojkova J, Zhou Y, Wong DF *et al* (2013) Memory decline shows stronger associations with estimated spatial patterns of amyloid deposition progression than total amyloid burden. *Neurobiology of Aging* **34**:2835–2842.
86. Zaidi H (2000) Comparative evaluation of scatter correction techniques in 3D positron emission tomography. *Eur J Nuclear Med* **27**:1813–1826.
87. Zaidi H, Montandon ML, Meikle S (2007) Strategies for attenuation compensation in neurological PET studies. *Neuroimage* **34**:518–541.
88. Ziolko SK, Weissfeld LA, Klunk WE, Mathis CA, Hoge JA, Lopresti BJ *et al* (2006) Evaluation of voxel-based methods for the statistical analysis of PIB PET amyloid imaging studies in Alzheimer's disease. *Neuroimage* **33**:94–102.